Probing the intergalactic magnetic field through gamma-ray observations with the Fermi LAT and H.E.S.S.

Manuel Meyer for the H.E.S.S. and Fermi LAT collaborations
manuel.meyer@uni-hamburg.de
Gamma 2022 Symposium, Barcelona, July 6, 2022

The Intergalactic magnetic field

IllustrisTNG simulation — Marinacci et al. (2018)

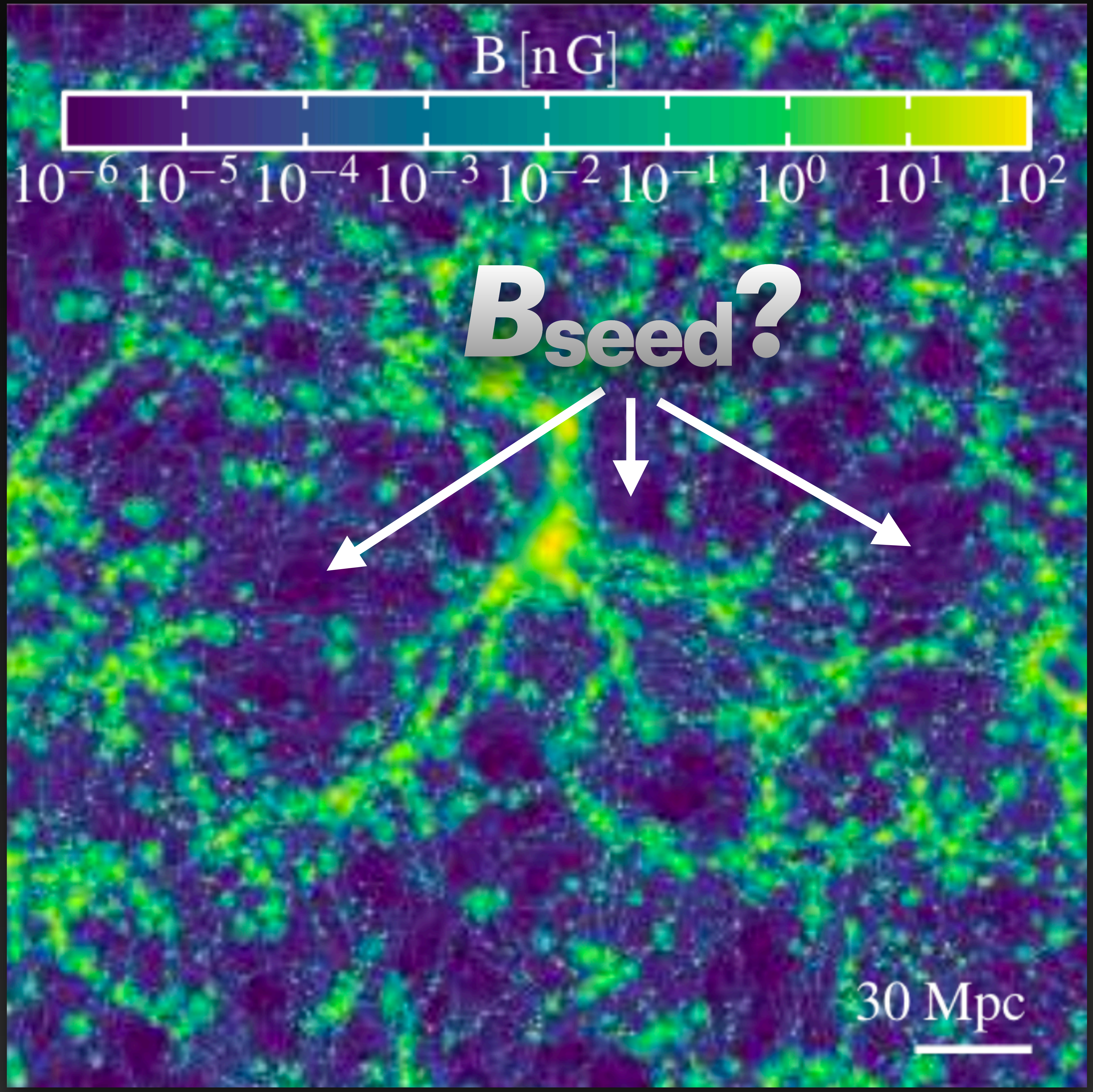

The Intergalactic magnetic field

- B-fields in galaxies and galaxy clusters originate from amplified seed field
- Origin, strength, orientation of seed fields unknown
- Extremely difficult to measure directly

IllustrisTNG simulation — Marinacci et al. (2018)

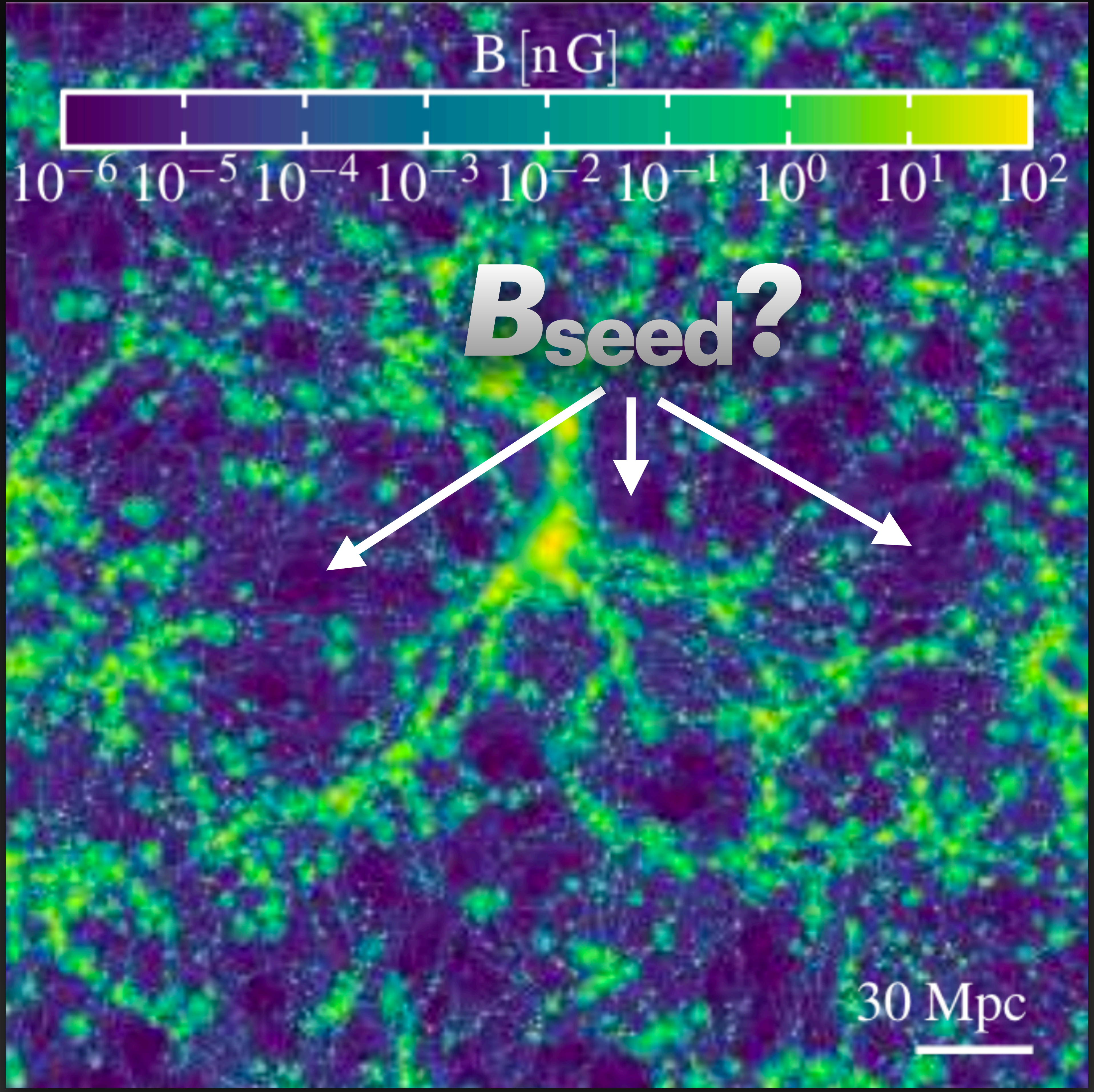

H.E.S.S.

Indirect detection of the IGMF

Using gamma-ray observations of blazars

- Excess γ rays at lower energies
  [e.g. Neronov & Semikoz 2008]
- Extended γ-ray halos
  [Aharonian et al. 1994]
- Time delayed γ-ray emission
  [Plaga 1995]
- Biggest uncertainty: blazar duty cycle
  [Dermer et al. 2011]

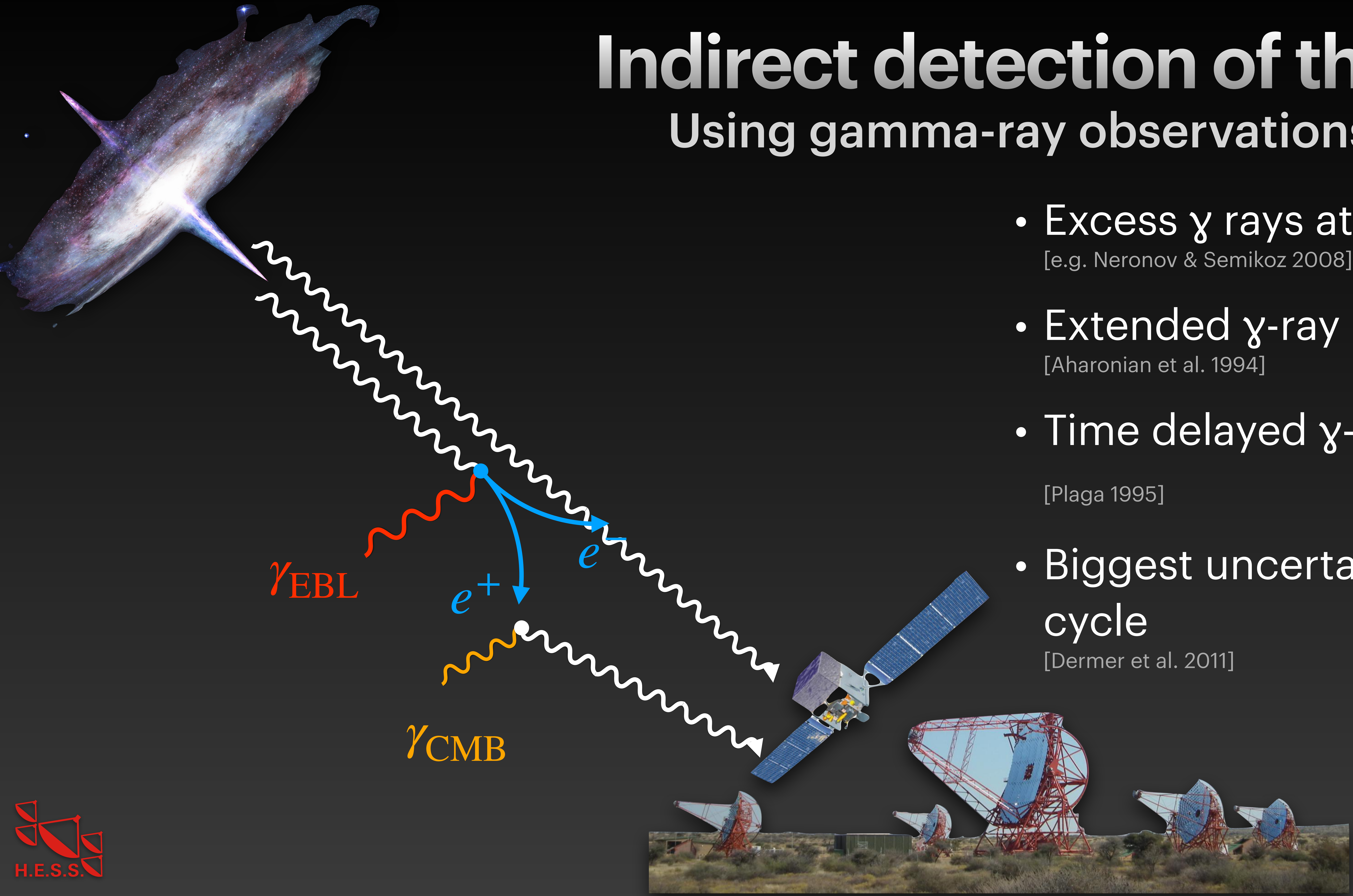

H.E.S.S.

Goal: new constraints on the IGMF

Using a combined maximum likelihood approach of H.E.S.S. and LAT data

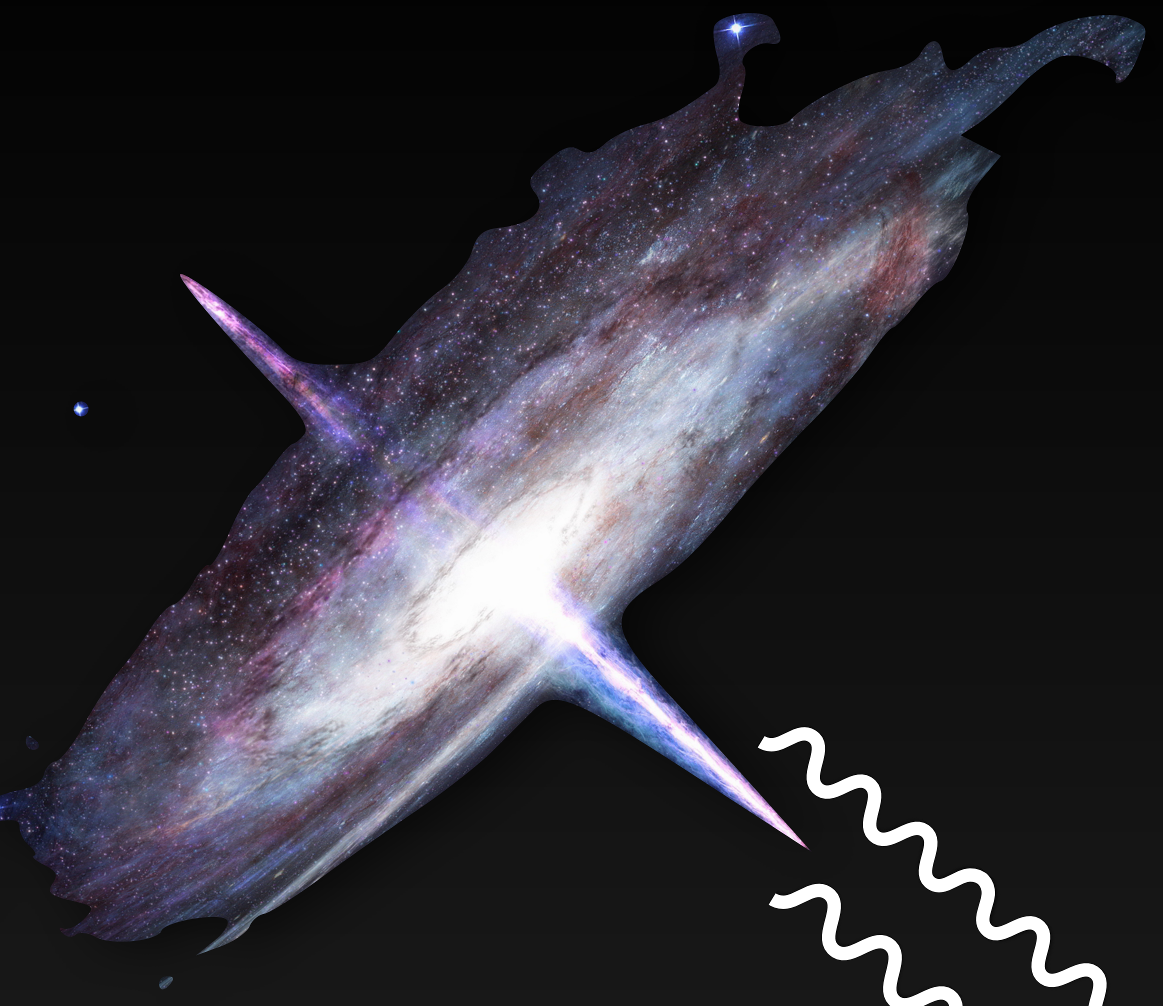

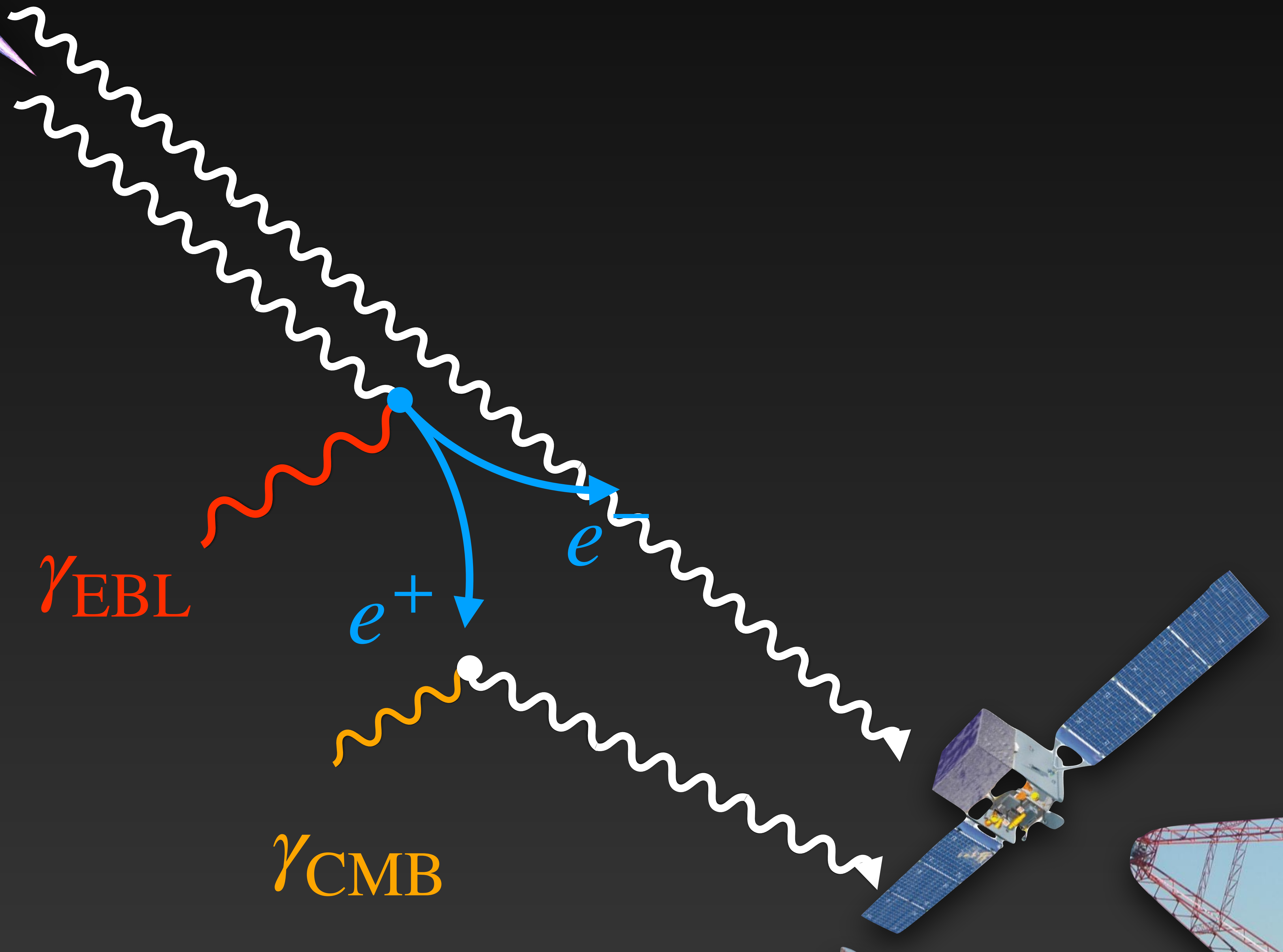

- Search for spatial and spectral halo signature
- Realistic predictions for halo from Monte Carlo Simulations
- Combining H.E.S.S. and Fermi-LAT data on the likelihood level

H.E.S.S.

Source Selection

- **Demands**:
  - Emission at energies corresponding to high optical depth
  - Stable gamma-ray emission in time as seen with the LAT
  - $\Rightarrow$ extreme HBL sources
- **Source selection from 4LAC-DR2 catalog**:
  - Spectral type: power law & $\Gamma + \sigma_\Gamma < 2$
  - Redshift known
  - BL Lac source type with synchrotron peak $\nu_{\mathrm{Sync}} > 10^{17}\,\mathrm{Hz}$
  - Chance probability < 99% that source is variable
  - Sources with TeV counterpart observed with H.E.S.S.

Resulting sources:

Source Name	Redshift
1ES 0229+200	0,139
1ES 0347-121	0,188
PKS 0548-322	0,069
1ES 1101-232	0,186
H 2356-309	0,165

H.E.S.S.

Modeling the halo with CRPropa3

- CRPropa 3 Monte Carlo Code used to generate 4D (spatial + energy + delay time) halo templates
- All relevant particle interactions included
- Halo templates generated for all sources for $B = 10^{-16}\,\mathrm{G}, \ldots, 10^{-13}\,\mathrm{G}$ for $\lambda_B = 1\,\mathrm{Mpc}$ and EBL model of Dominguez et al. (2011)
- Developed python wrapper in order to:
    - Reweight simulations for different input spectra [Ackermann et al. 2018]
    - Smooth sky maps adaptively [Ebeling et al. 2006]
    - Change orientation between source and observer in post processing [Alves Batista et al. 2016]
    - Change blazar activity time

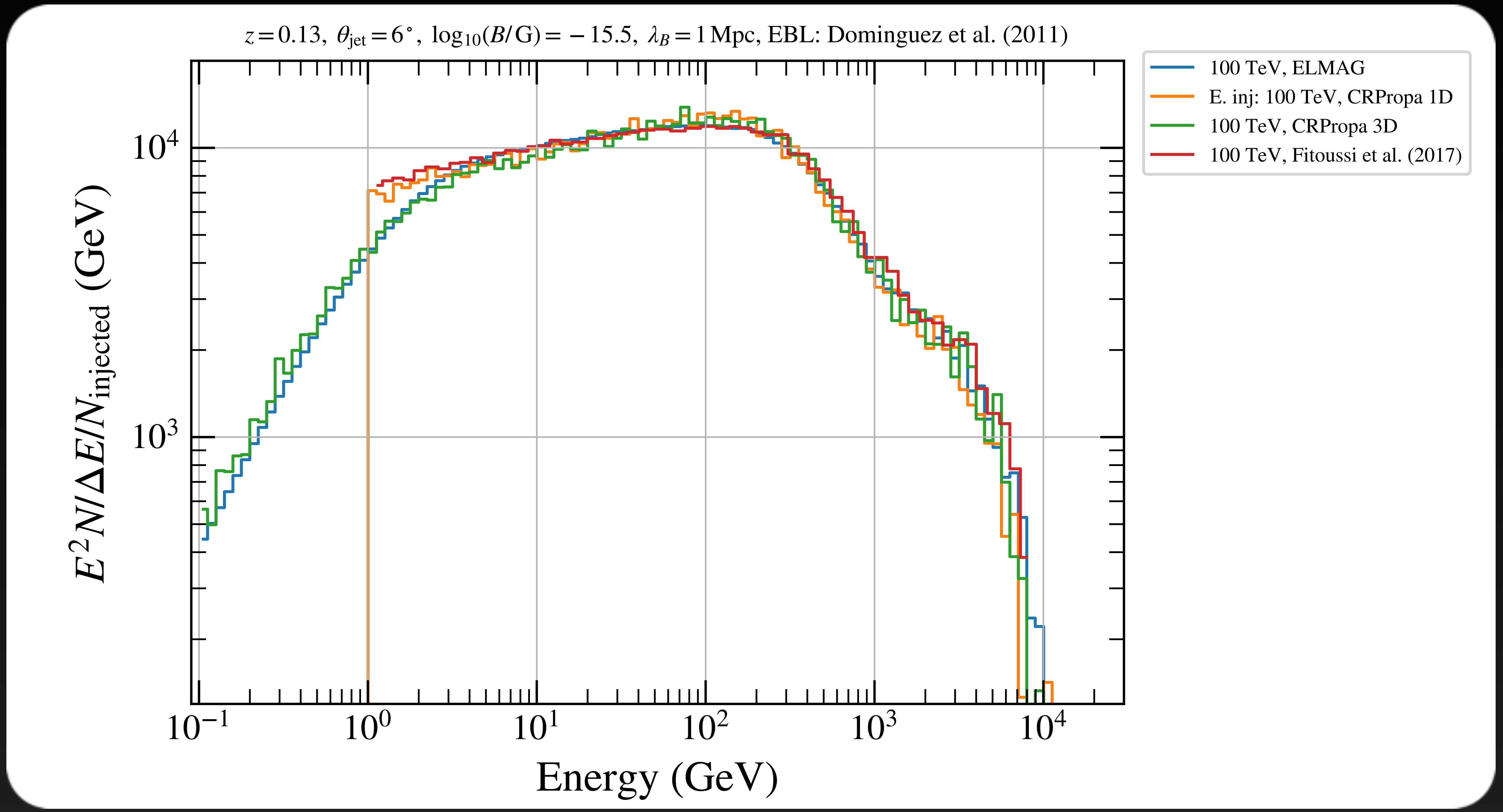

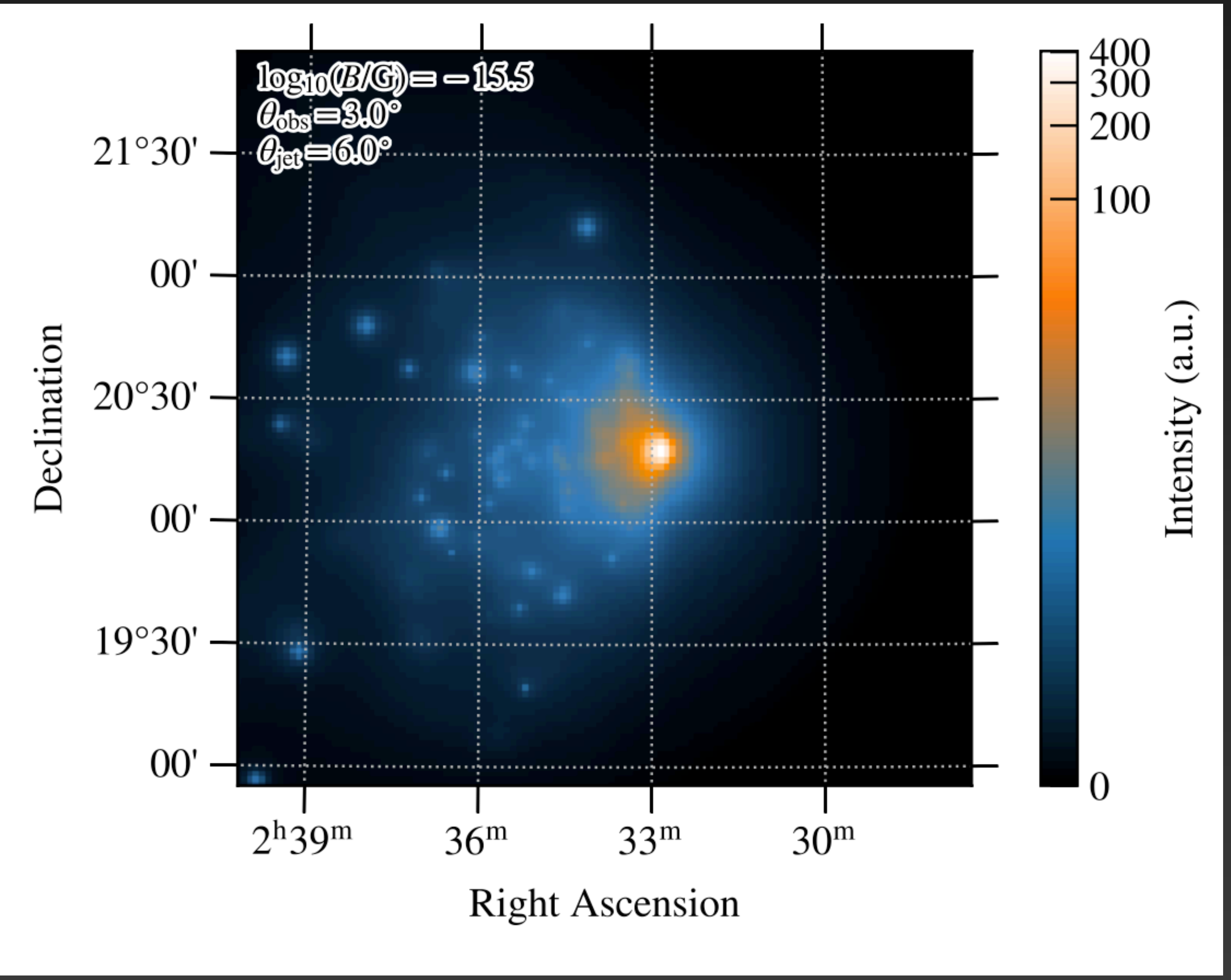

Fermi-LAT data selection

Parameter	Selection
Time range	11.5 years
Energy Range	> 1 GeV
ROI size	6º x 6º
Max. Zenith angle	100º
Filter	DATA_QUAL>0 && LAT_CONFIG==1
Spatial binning	0.025º / pixel
Energy binning	8 bins per decade
Event Class / IRFs	P8R3_SOURCE_V3, inflight PSF
Event types	PSF0-2, PSF3

Extracting LAT likelihoods in the presence of a halo

- First step: standard LAT point source analysis
- Source spectrum: $\phi_{\rm obs} = N(E/E_0)^{-\Gamma}\exp(-\tau)$
- Sources appear well described by point sources
- For each simulated IGMF strength:
  - Change point source model to $\phi_{\rm obs} = N(E/E_0)^{-\Gamma}\exp(-E/E_{\rm cut})\exp(-\tau)$
  - Loop over spectral parameters, add corresponding halo template, extract likelihood of fit, $\ln \mathscr{L}_{\rm LAT}$

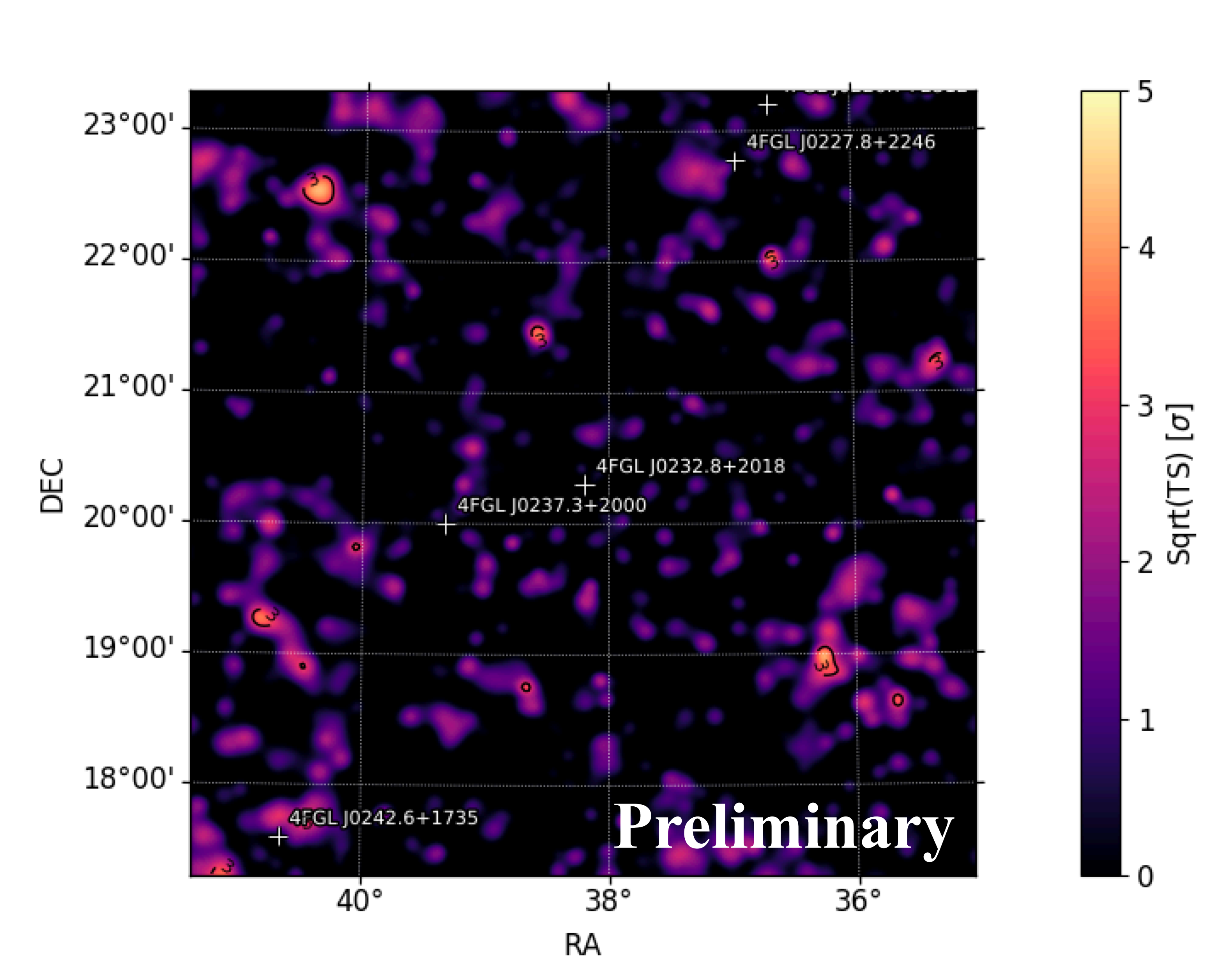

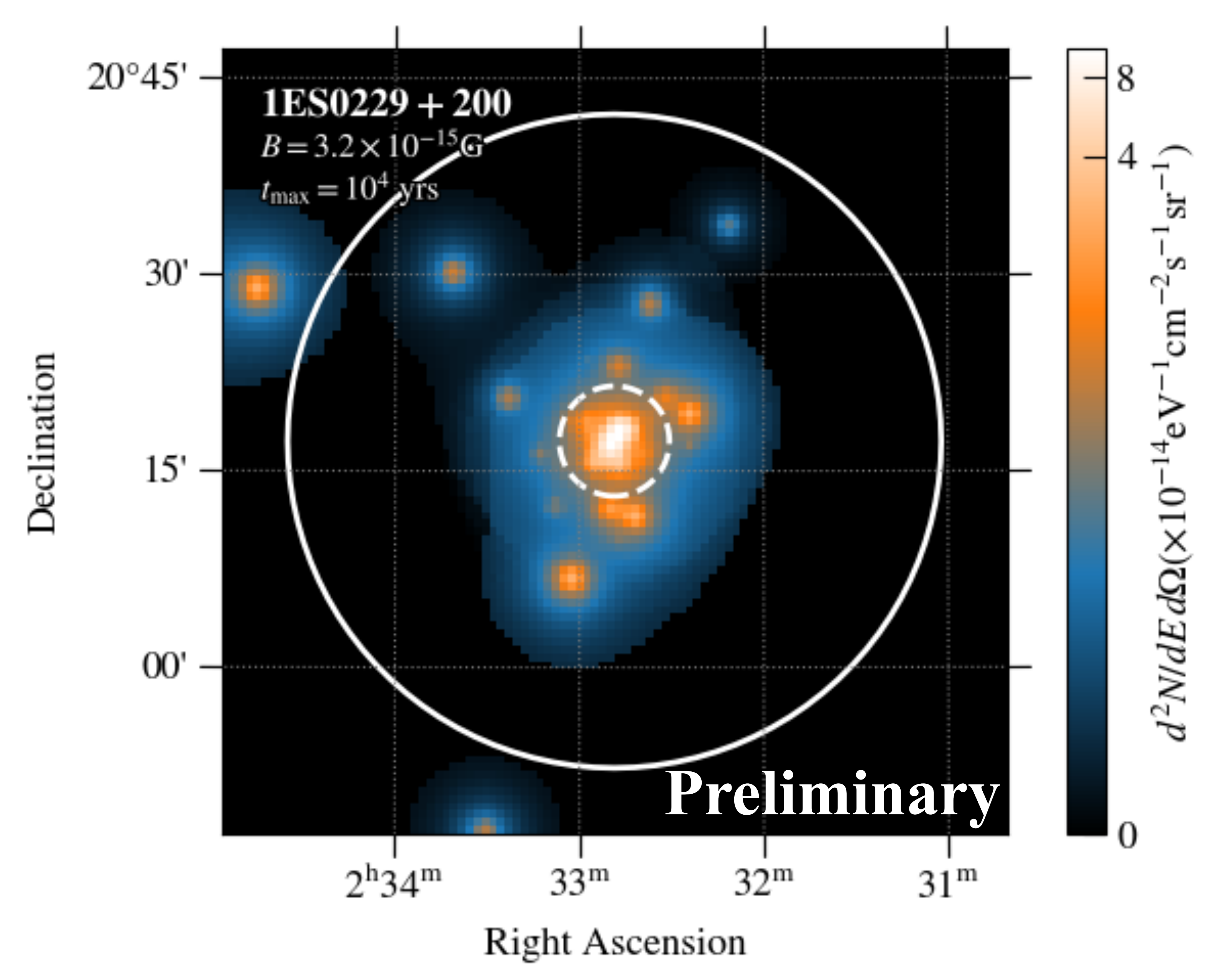

H.E.S.S.

H.E.S.S. Data sets

- Data taken with small telescopes up to 2018 considered here
- Analysis performed using gammapy [Deil et al. 2017]
- Source spectra $\phi_{\rm obs}$ well described by power law including EBL absorption, $\phi_{\rm obs} = N(E/E_0)^{-\Gamma}\exp(-\tau)$

Preliminary

Source	Life time (hours)	Detection significance	Power law index Γ
1ES 0229+200	144,1	16.5σ	1.76 ± 0.12
1ES 0347-121	59,2	16.1σ	2.12 ± 0.15
PKS 0548-322	53,9	10.2σ	1.92 ± 0.12
1ES 1101-232	71,9	18.7σ	1.66 ± 0.09
H 2356-309	150,5	23.4σ	2.10 ± 0.09

H.E.S.S.

Combined H.E.S.S. and LAT analysis

- Intrinsic blazar model:

$$\phi(E) = N\left(\frac{E}{E_0}\right)^{-\Gamma} \exp\left(-\frac{E}{E_{\mathrm{cut}}}\right)$$

- Total source model:

$$\phi_{\mathrm{tot}}(E,B) = \phi(E)\exp(-\tau) + \phi_{\mathrm{halo}}(E,B)$$

- Halo flux taken from CRPropa3 simulation; depends on spectral parameters, blazar activity time...

- Spectral parameters optimized using combined H.E.S.S. and LAT likelihoods:

$$\ln \mathscr{L} = \ln \mathscr{L}_{\mathrm{LAT}} + \ln \mathscr{L}_{\mathrm{H.E.S.S.}}$$

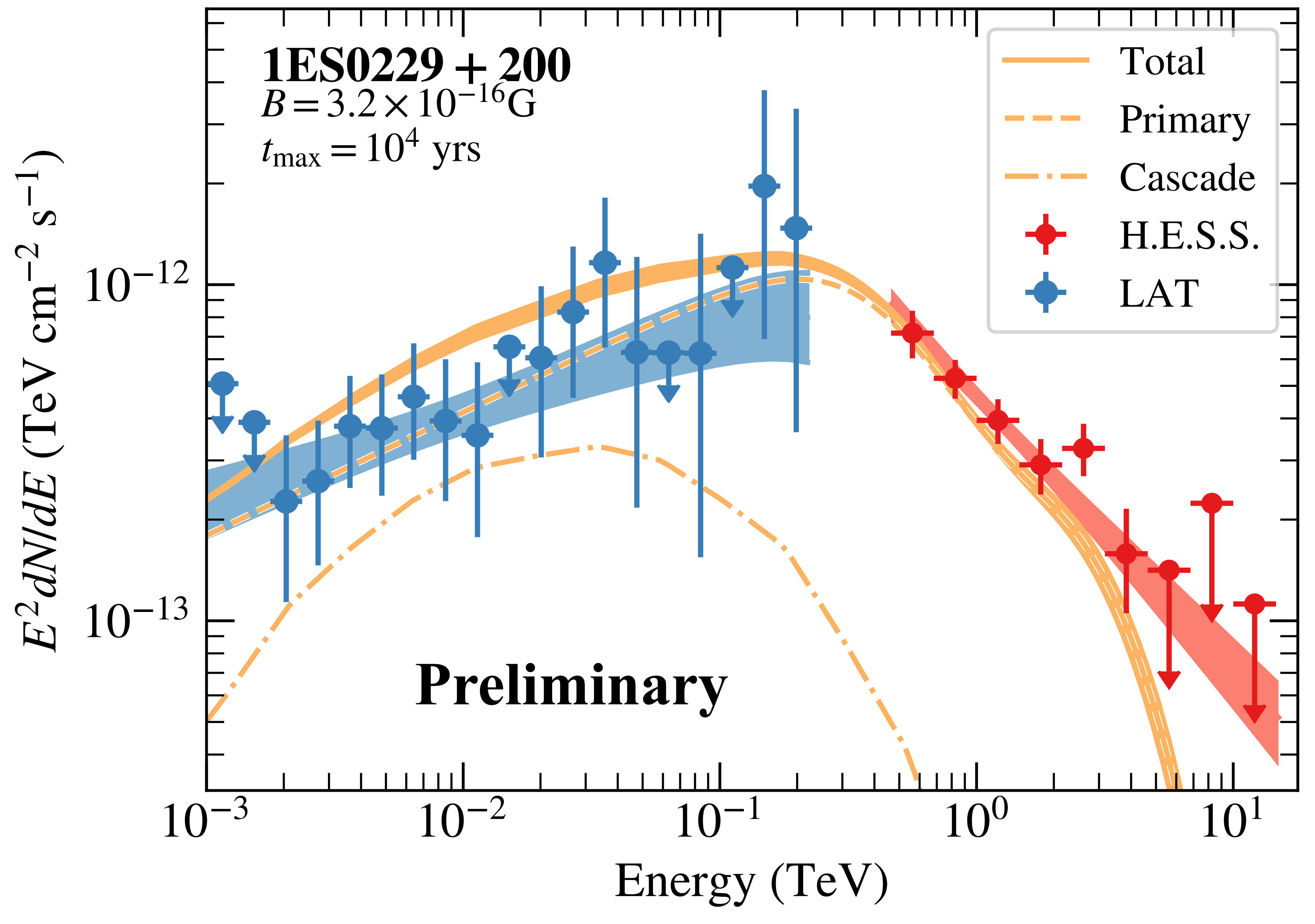

H.E.S.S.

Combined H.E.S.S. and LAT analysis

- Intrinsic blazar model:

$$\phi(E) = N\left(\frac{E}{E_0}\right)^{-\Gamma} \exp\left(-\frac{E}{E_{\rm cut}}\right)$$

- Total source model:

$$\phi_{\rm tot}(E,B) = \phi(E)\exp(-\tau) + \phi_{\rm halo}(E,B)$$

- Halo flux taken from CRPropa3 simulation; depends on spectral parameters, blazar activity time…

- Spectral parameters optimized using combined H.E.S.S. and LAT likelihoods:

$$\ln \mathscr{L} = \ln \mathscr{L}_{\rm LAT} + \ln \mathscr{L}_{\rm H.E.S.S.}$$

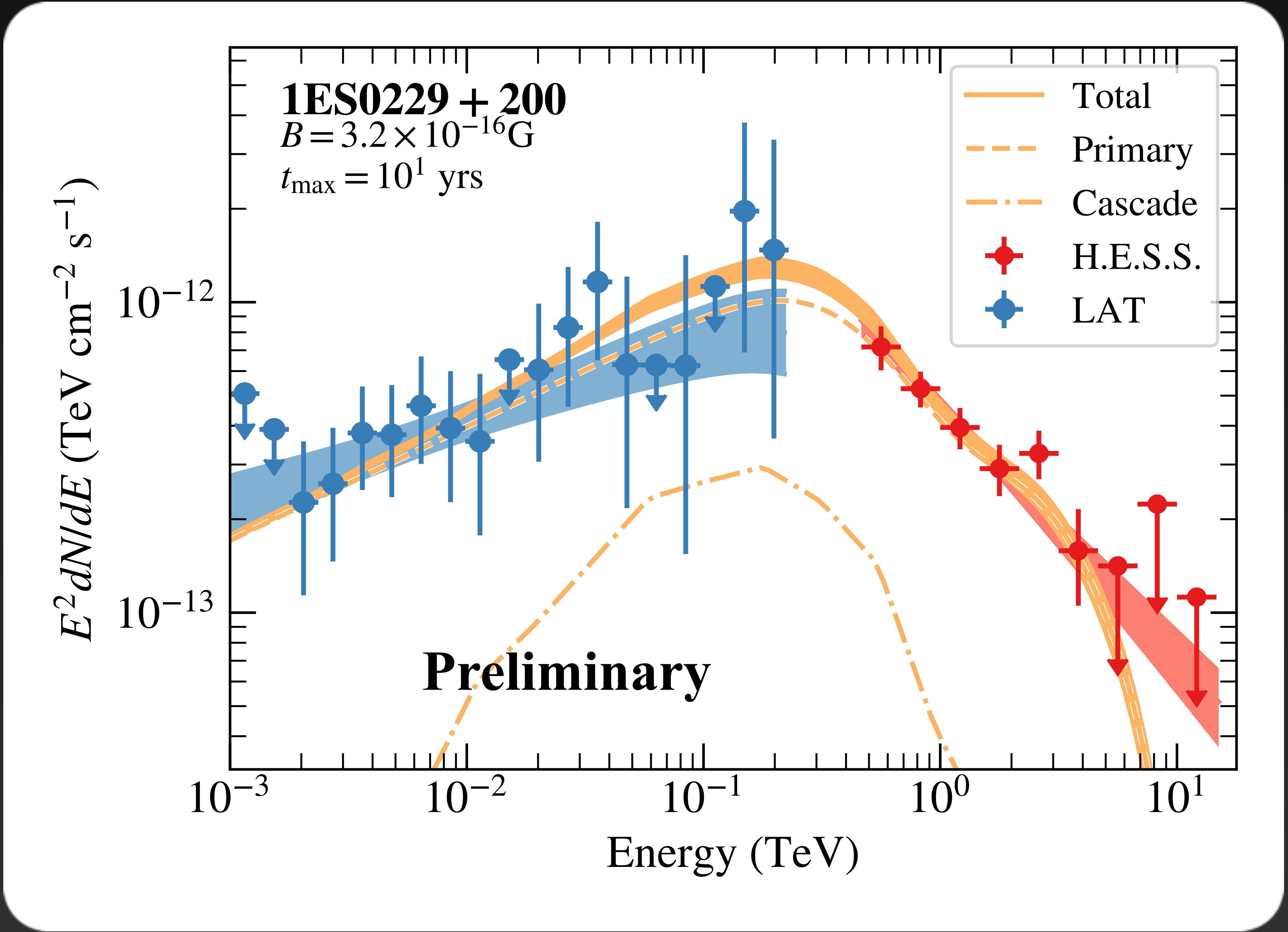

H.E.S.S.

Combined H.E.S.S. and LAT analysis

- Intrinsic blazar model:

$$\phi(E) = N\left(\frac{E}{E_0}\right)^{-\Gamma} \exp\left(-\frac{E}{E_{cut}}\right)$$

- Total source model:

$$\phi_{tot}(E,B) = \phi(E)\exp(-\tau) + \phi_{halo}(E,B)$$

- Halo flux taken from CRPropa3 simulation; depends on spectral parameters, blazar activity time…

- Spectral parameters optimized using combined H.E.S.S. and LAT likelihoods:

$$\ln \mathscr{L} = \ln \mathscr{L}_{LAT} + \ln \mathscr{L}_{H.E.S.S.}$$

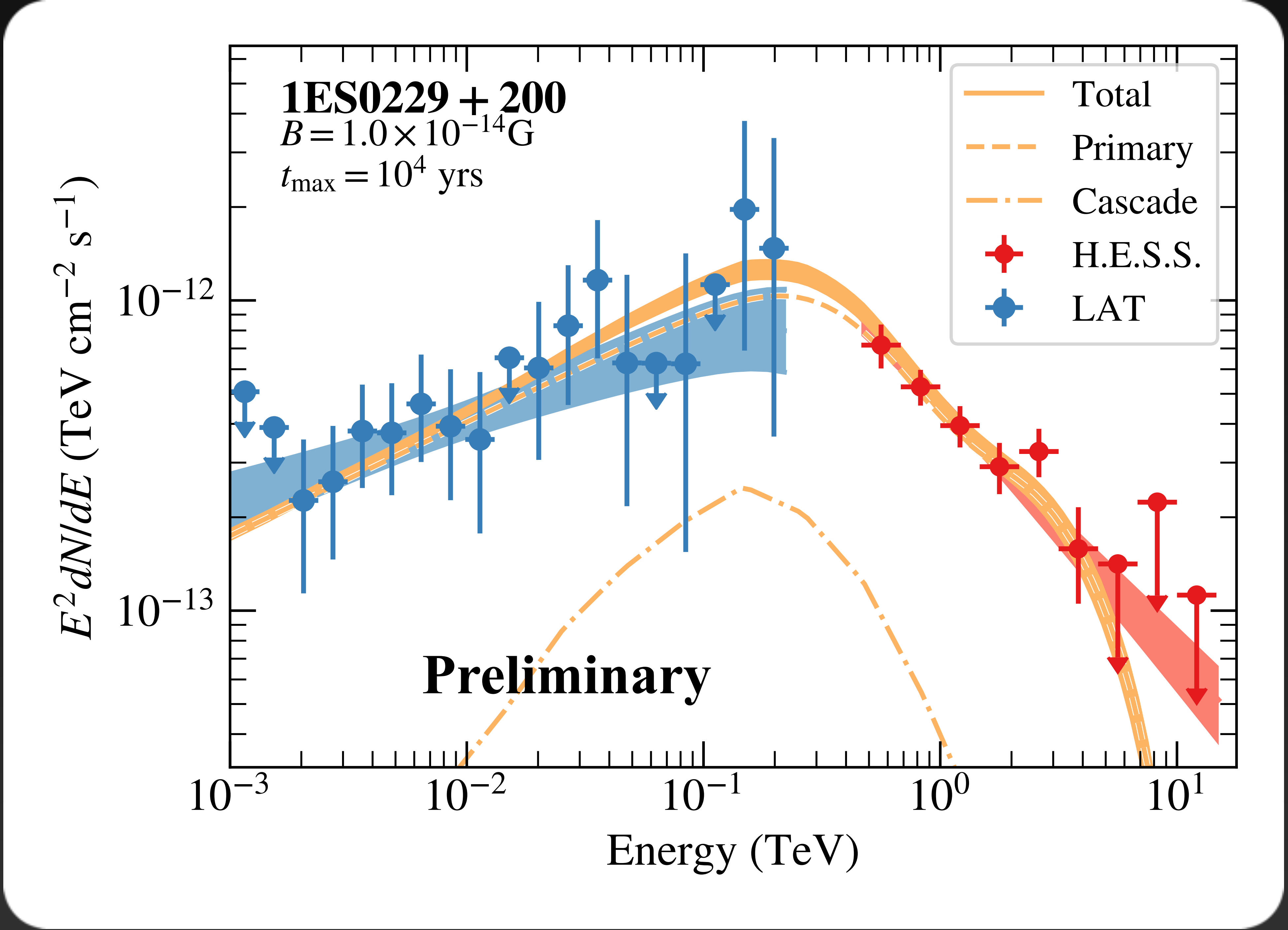

H.E.S.S.

Results: lower limits on IGMF

Data does not prefer presence of halo

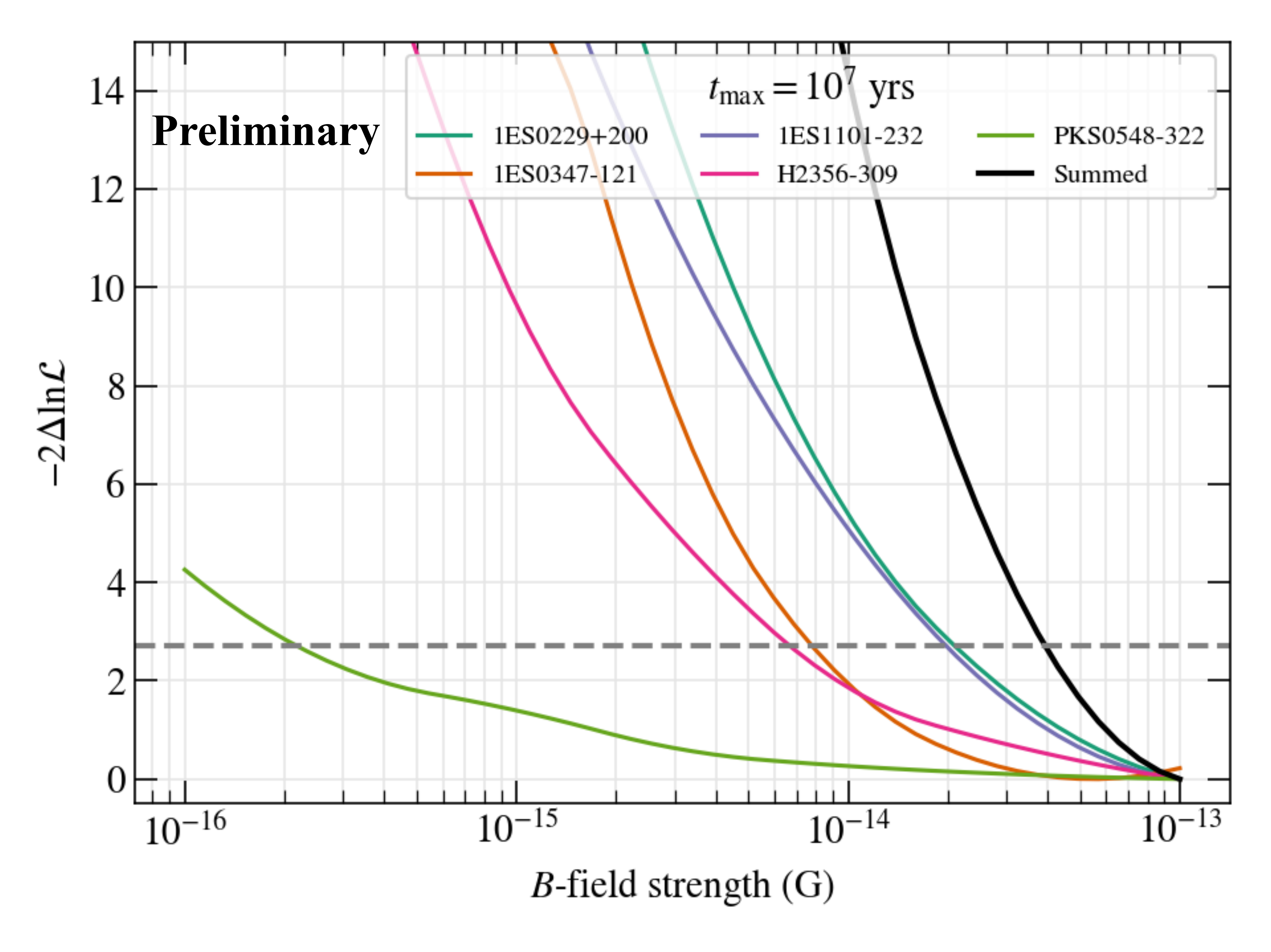

H.E.S.S.

Results: lower limits on IGMF

Data does not prefer presence of halo

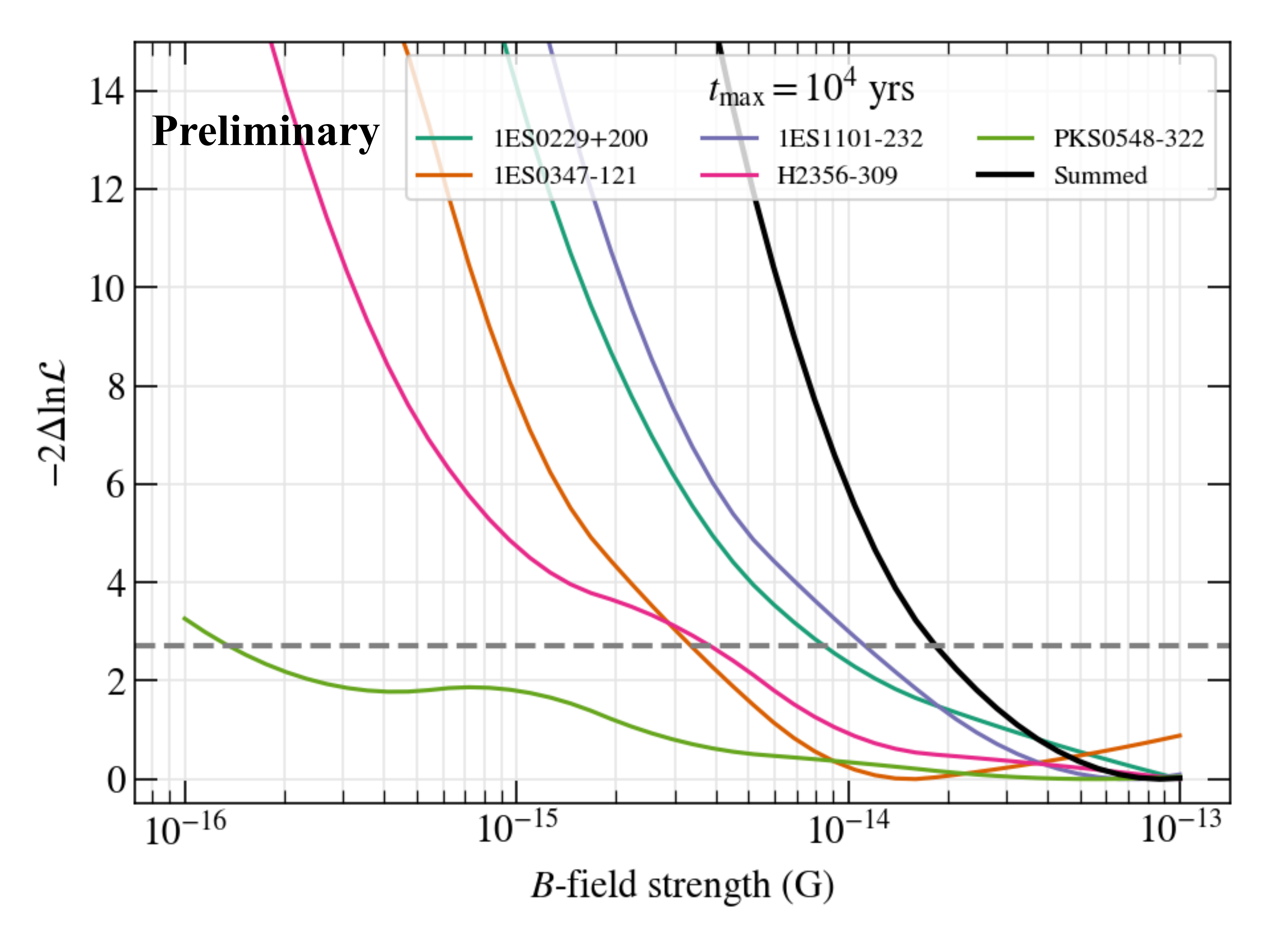

Results: lower limits on IGMF

Data does not prefer presence of halo

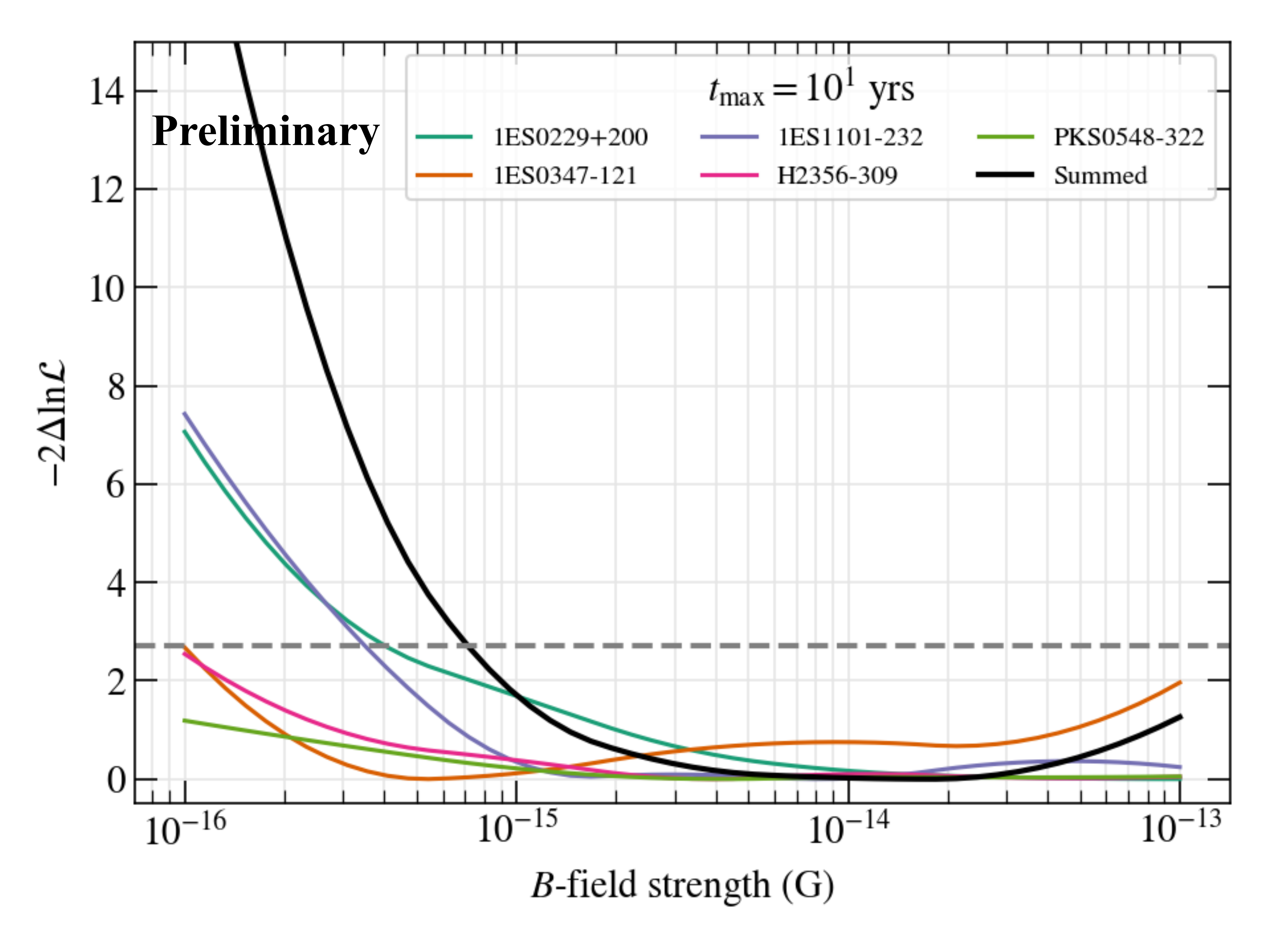

H.E.S.S.

Conclusions

- `CRPropa3` simulations used to generate realistic cascade templates
- Combination LAT and H.E.S.S. data rules out B fields weaker than $B \lesssim 7 \times 10^{-16}\,\mathrm{G}$ for $t_{\mathrm{max}} = 10\,\mathrm{yr}$
- Previous constraints improved by factor of 2

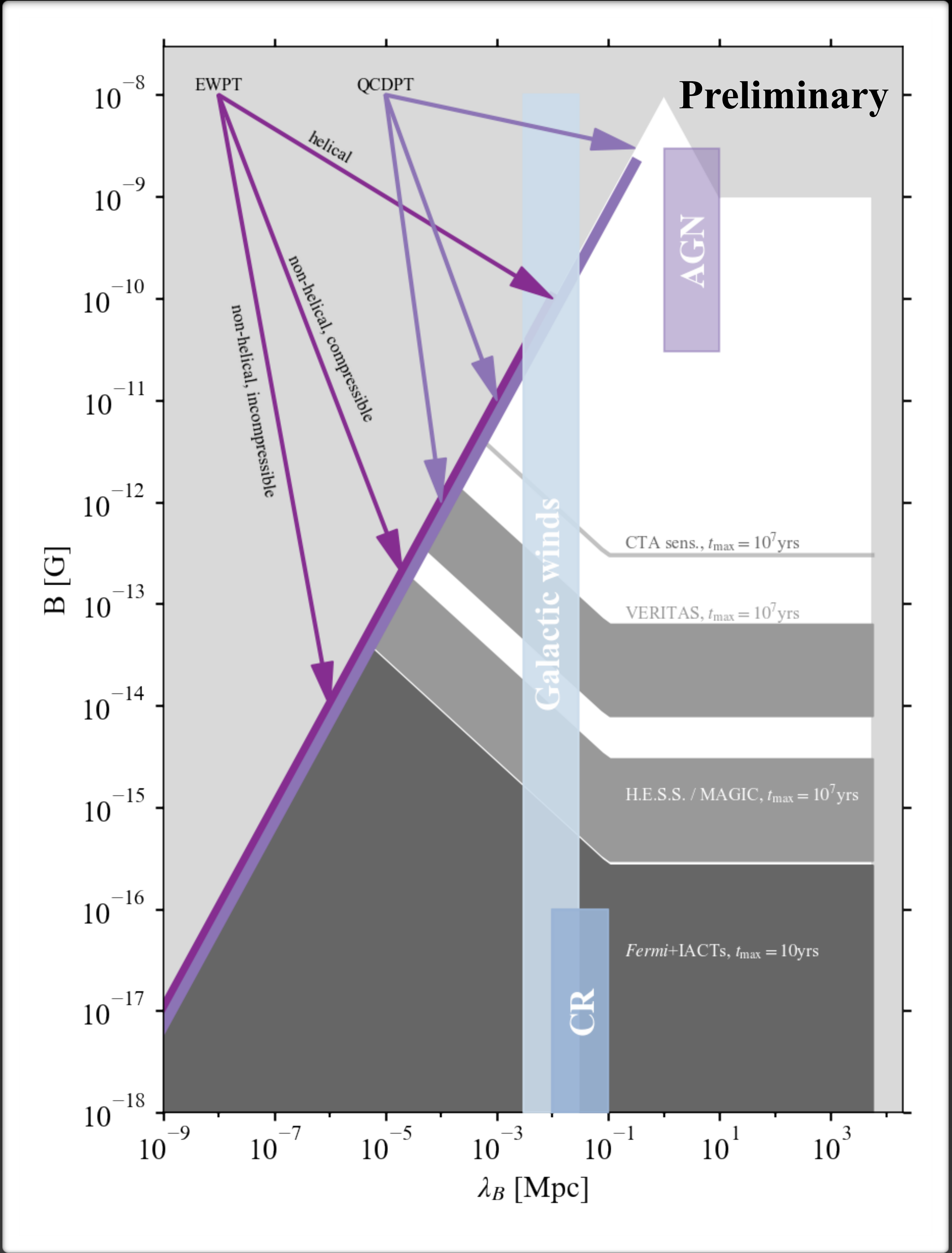

[Adapted from Durrer & Neronov 2013 and Abdalla et al. 2021]

H.E.S.S.

Conclusions

- `CRPropa3` simulations used to generate realistic cascade templates
- Combination LAT and H.E.S.S. data rules out B fields weaker than $B \lesssim 7 \times 10^{-16}\,\mathrm{G}$ for $t_{\mathrm{max}} = 10\,\mathrm{yr}$
- Previous constraints improved by factor of 2

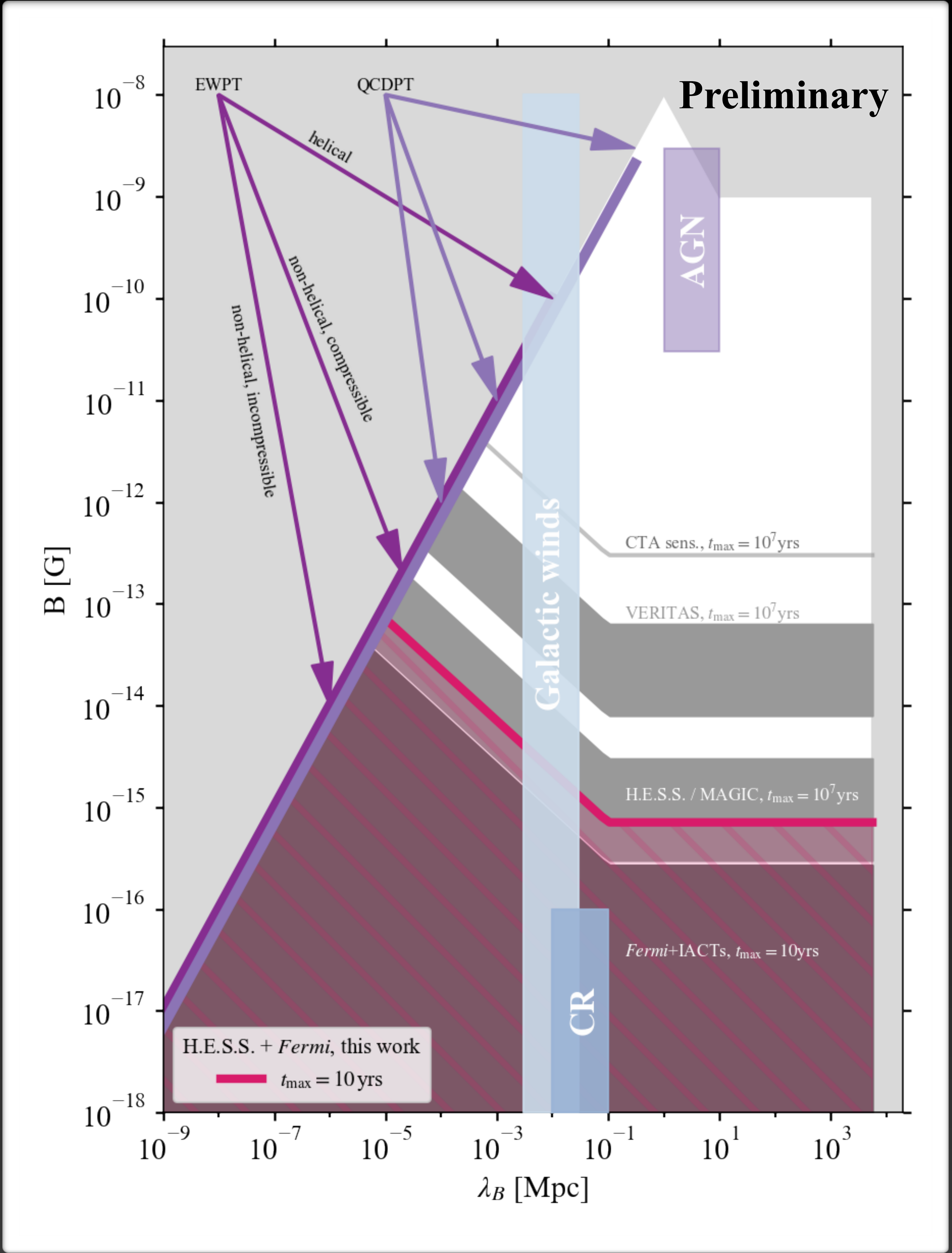

[Adapted from Durrer & Neronov 2013 and Abdalla et al. 2021]

H.E.S.S.

Conclusions

- `CRPropa3` simulations used to generate realistic cascade templates
- Combination LAT and H.E.S.S. data rules out B fields weaker than $B \lesssim 7 \times 10^{-16}\,\mathrm{G}$ for $t_{\max} = 10\,\mathrm{yr}$
- Previous constraints improved by factor of 2

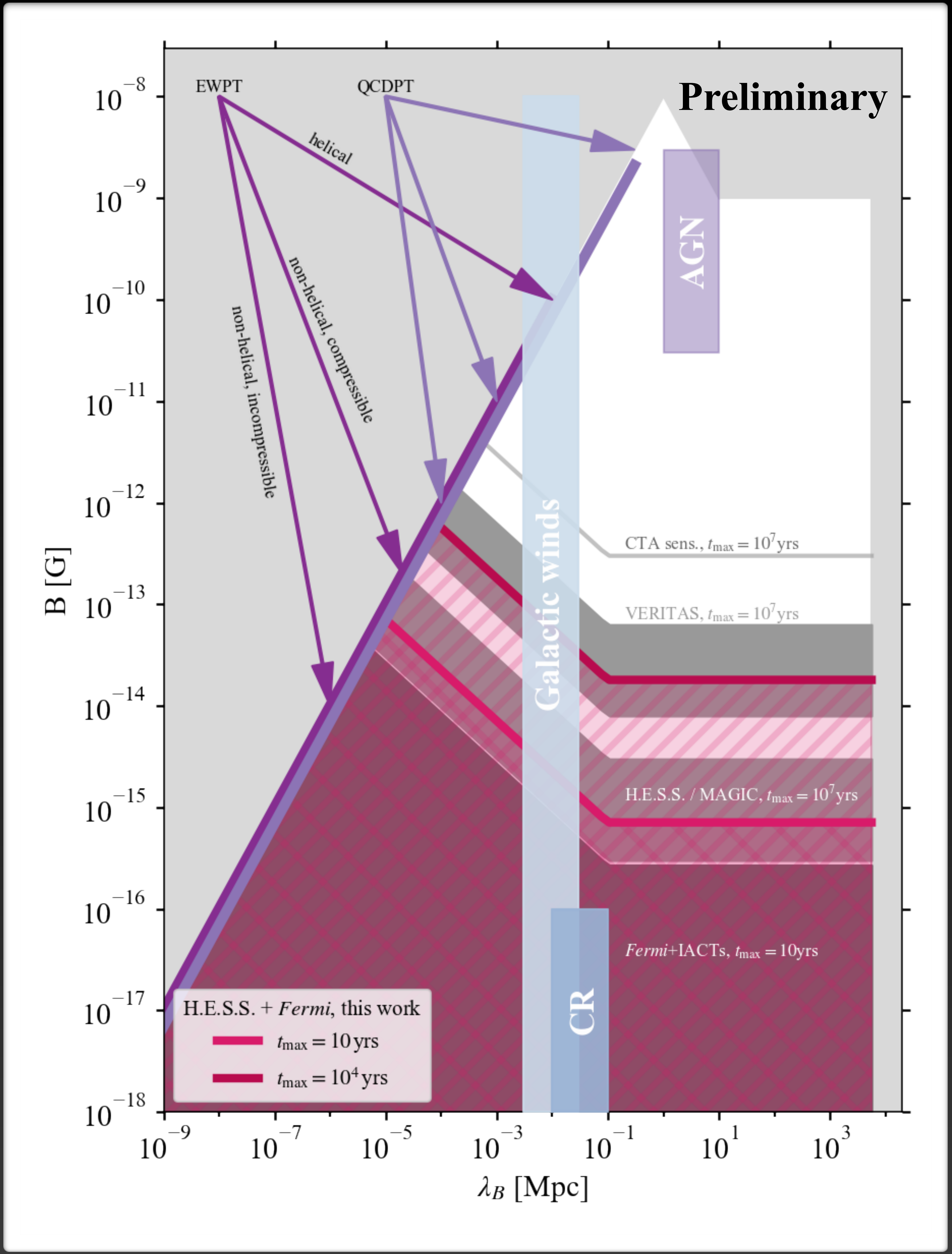

[Adapted from Durrer & Neronov 2013 and Abdalla et al. 2021]

H.E.S.S.

Conclusions

- `CRPropa3` simulations used to generate realistic cascade templates
- Combination LAT and H.E.S.S. data rules out B fields weaker than $B \lesssim 7 \times 10^{-16}\,\mathrm{G}$ for $t_{\mathrm{max}} = 10\,\mathrm{yr}$
- Previous constraints improved by factor of 2

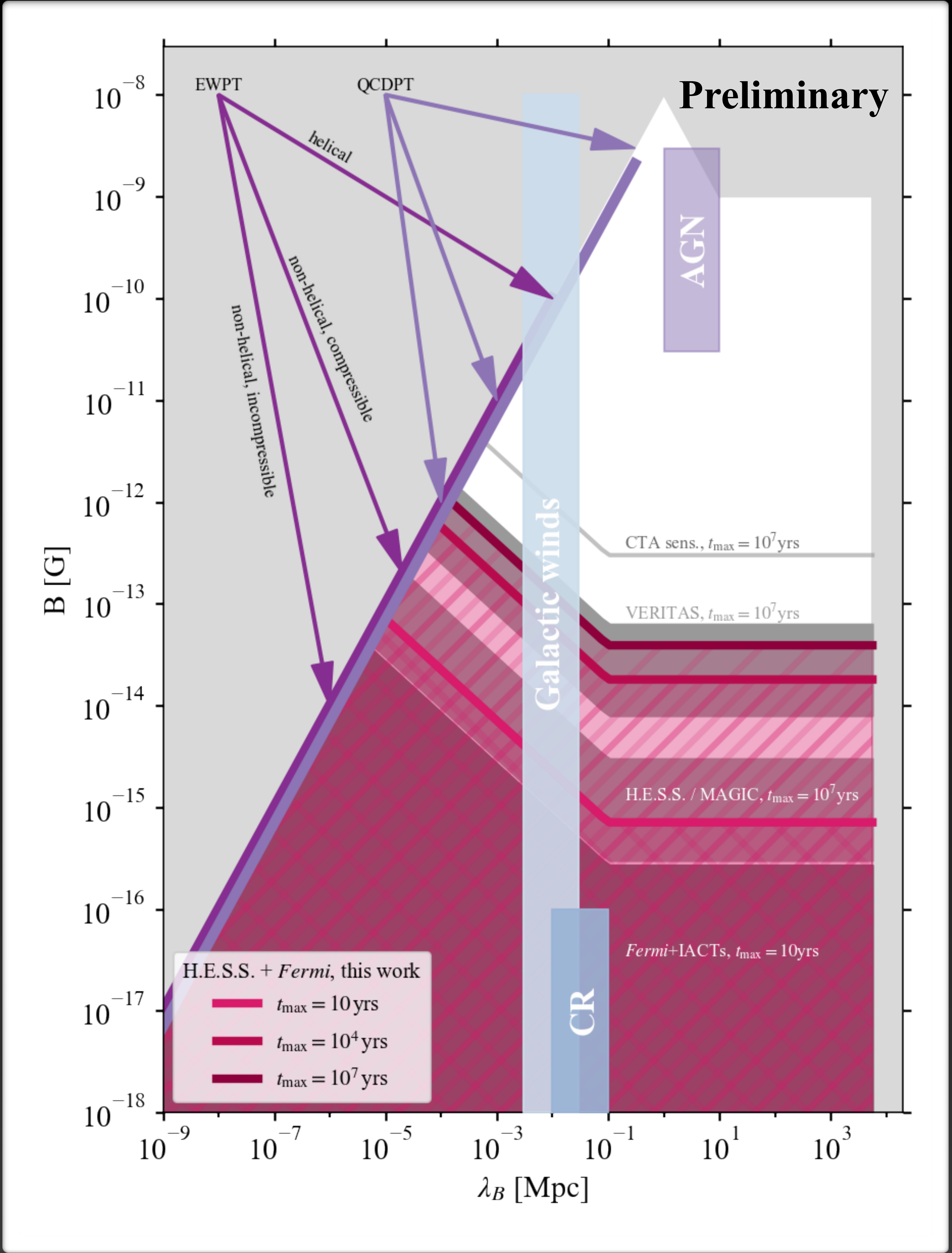

[Adapted from Durrer & Neronov 2013 and Abdalla et al. 2021]

H.E.S.S.

Back up

Fermi-LAT analysis with halo component

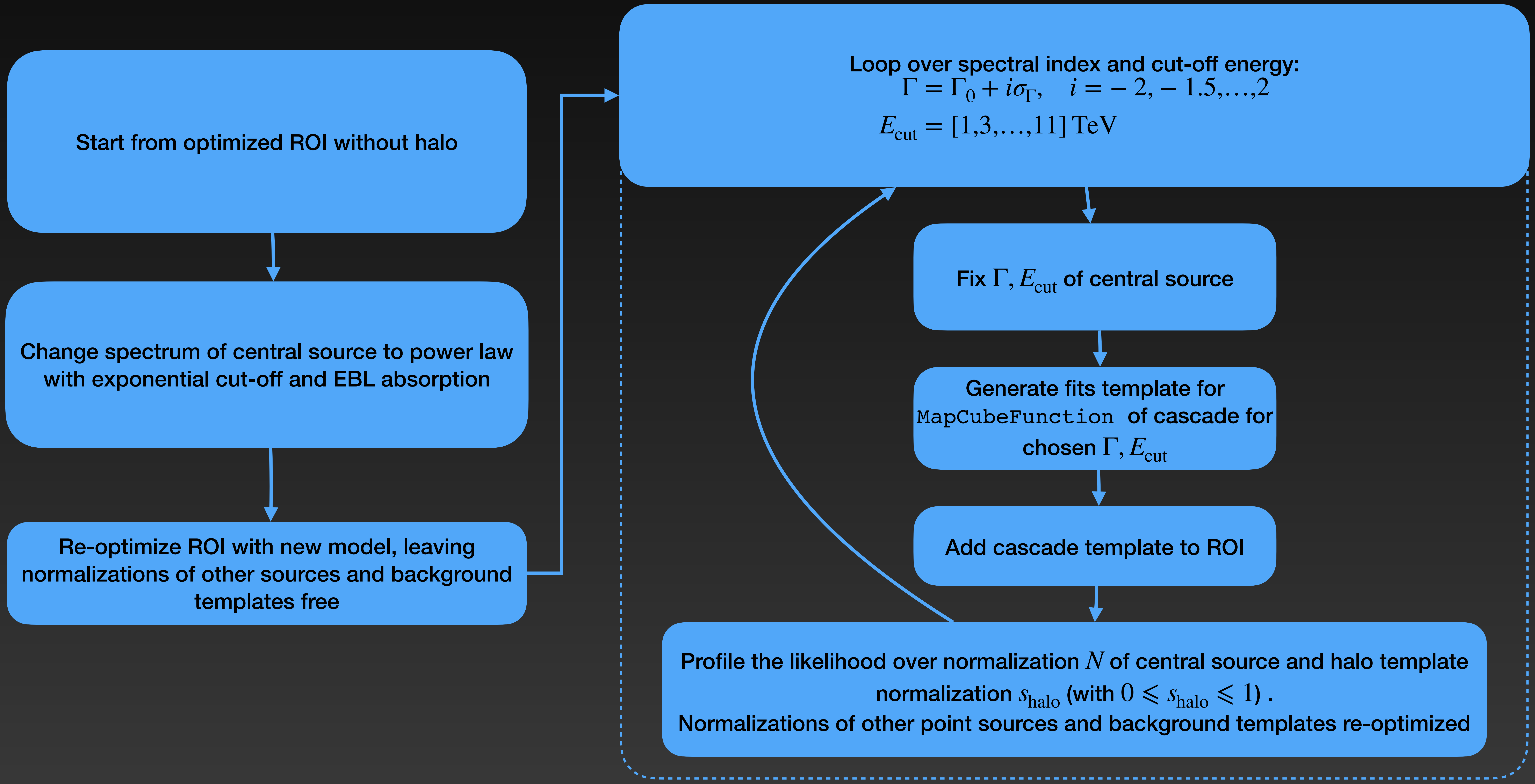

Building cascade templates

- From the simulated events we build the intensity as function of injected gamma-ray energy ϵ, observed energy E, solid Ω, and delay time τ:

$$\frac{d\mathcal{N}}{d\epsilon dE d\tau d\Omega} = \frac{1}{N_{\mathrm{inj}}(\Delta\epsilon)} \frac{\mathcal{N}}{\Delta E \Delta\epsilon \Delta\tau \Delta\Omega}$$

- Simulation done for discrete injection energies ϵ_i
- From this, we can re-weight the cascade histogram for an arbitrary source spectra $dN/d\epsilon$ (e.g., a power law), by computing weights for bins of injected energy:

$$w_i = \int_{\Delta\epsilon_i} \frac{dN}{d\epsilon} d\epsilon$$

- With the spectral weights, we obtain the expected cascade flux that arrives within some maximum time delay (assuming constant emission with time)

$$\frac{d\mathcal{N}}{dE d\Omega} = \int_0^\infty d\epsilon \frac{dN}{d\epsilon} \int_0^{\tau_{\max}} d\tau \frac{d\mathcal{N}}{d\epsilon dE d\tau d\Omega} \approx \sum_i \sum_j \Delta\epsilon_i \Delta\tau_j w_i \left(\frac{d\mathcal{N}}{d\epsilon dE d\tau d\Omega} \right)_{ij}$$

- Cascade flux will depend on IGMF strength B and coherence length λ, injection spectrum, maximum activity time of the source $t_{\max}$, as well as θ_{jet}, θ_{obs} and source redshift z

H.E.S.S.

Cascade templates as function of IGMF strength: sky maps

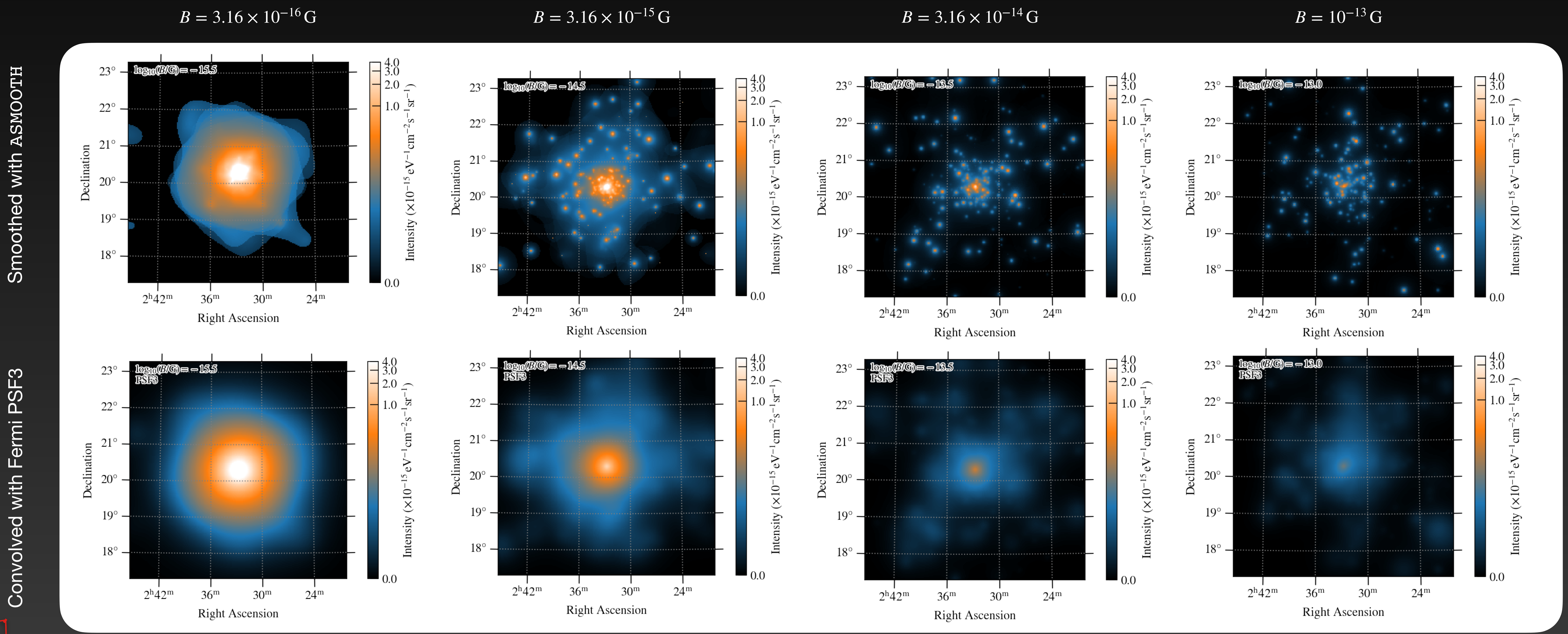

Cascade templates as function of IGMF strength: lon/lat profiles

$B = 3.16 \times 10^{-16}$ G, sky map summed over lon/lat and energy

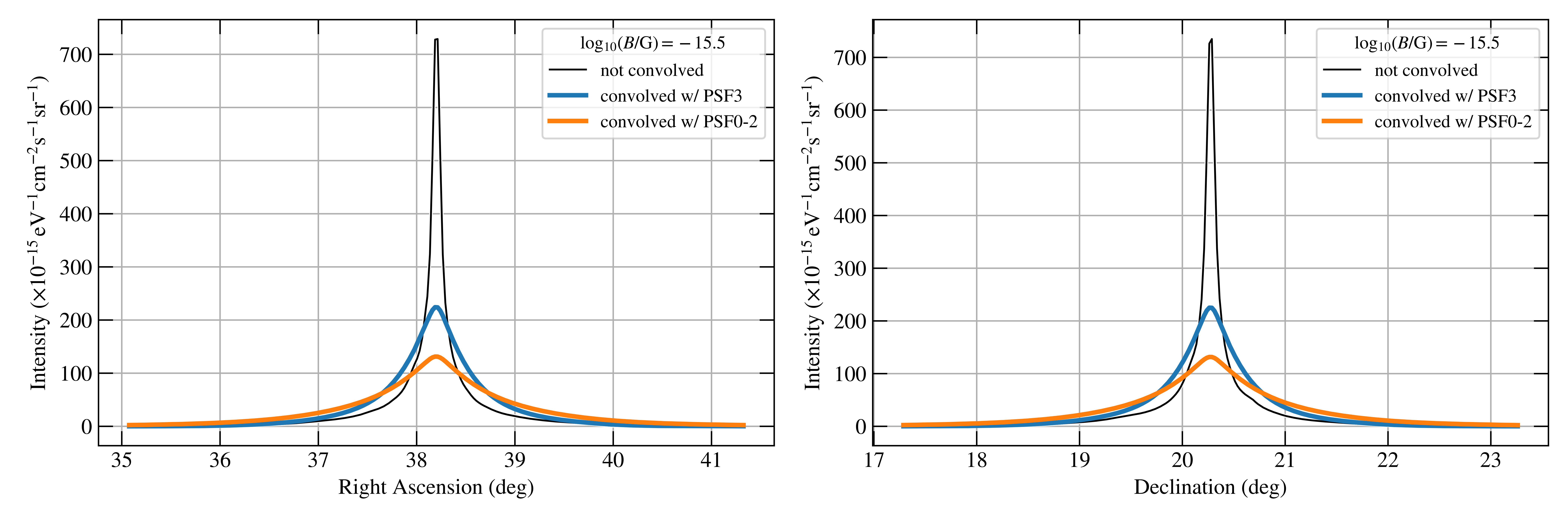

Cascade templates as function of IGMF strength: lon/lat profiles

$B = 3.16 \times 10^{-15}$ G, sky map summed over lon/lat and energy

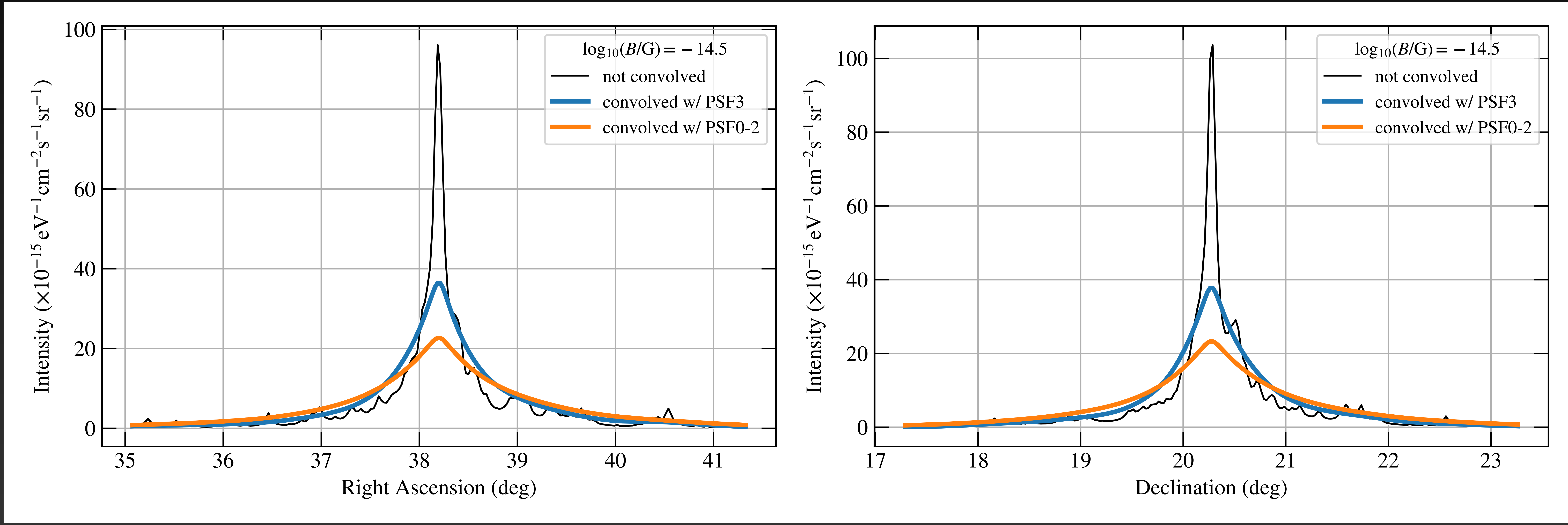

Cascade templates as function of IGMF strength: lon/lat profiles

$B = 3.16 \times 10^{-14}$ G, sky map summed over lon/lat and energy

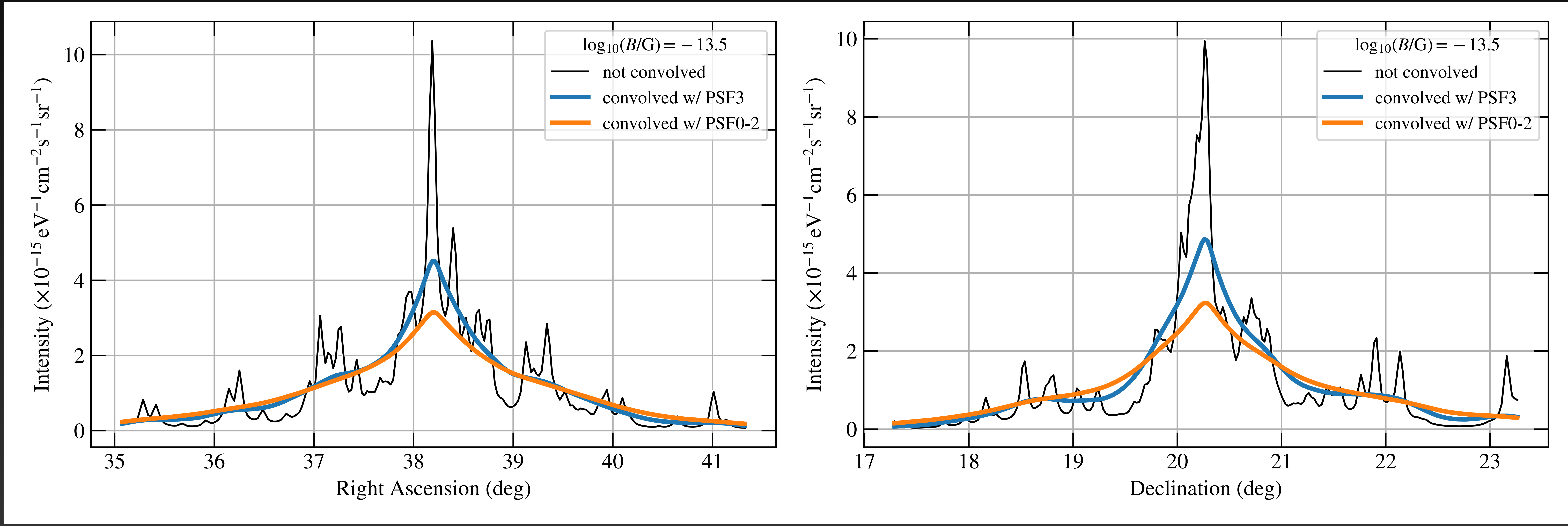

H.E.S.S.

Cascade templates as function of IGMF strength: lon/lat profiles

$B = 10^{-13}$ G, sky map summed over lon/lat and energy

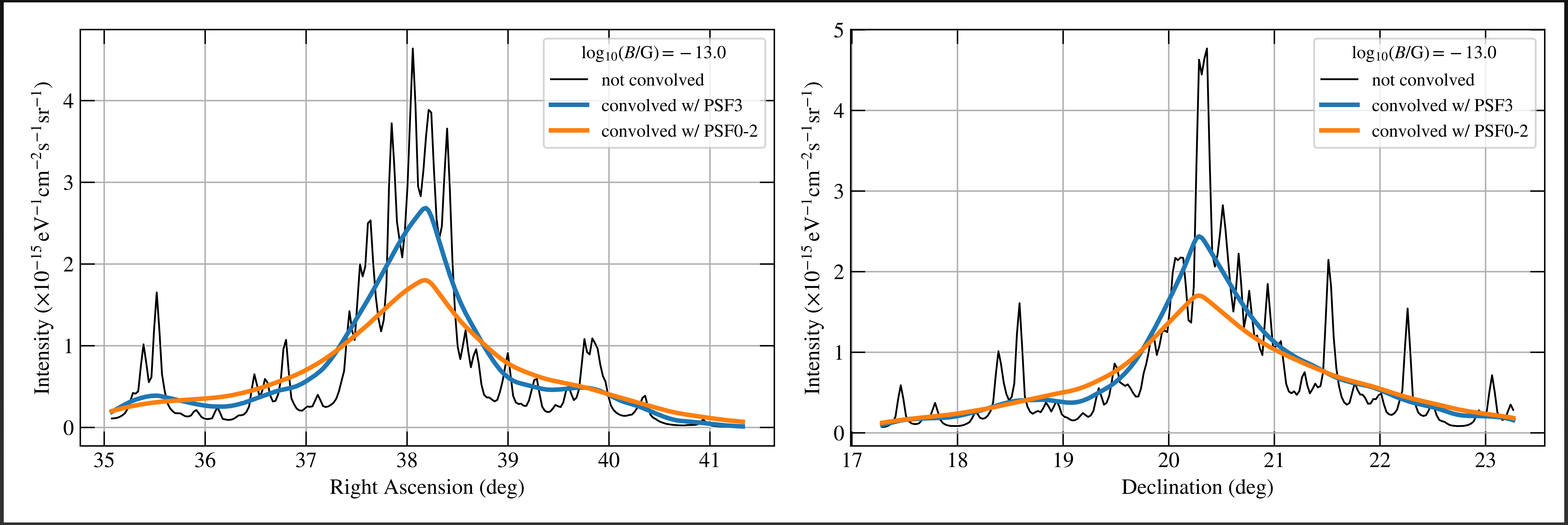

H.E.S.S.

Fermi-LAT Analysis with halo component — Examples of likelihood profile with E_{cut}

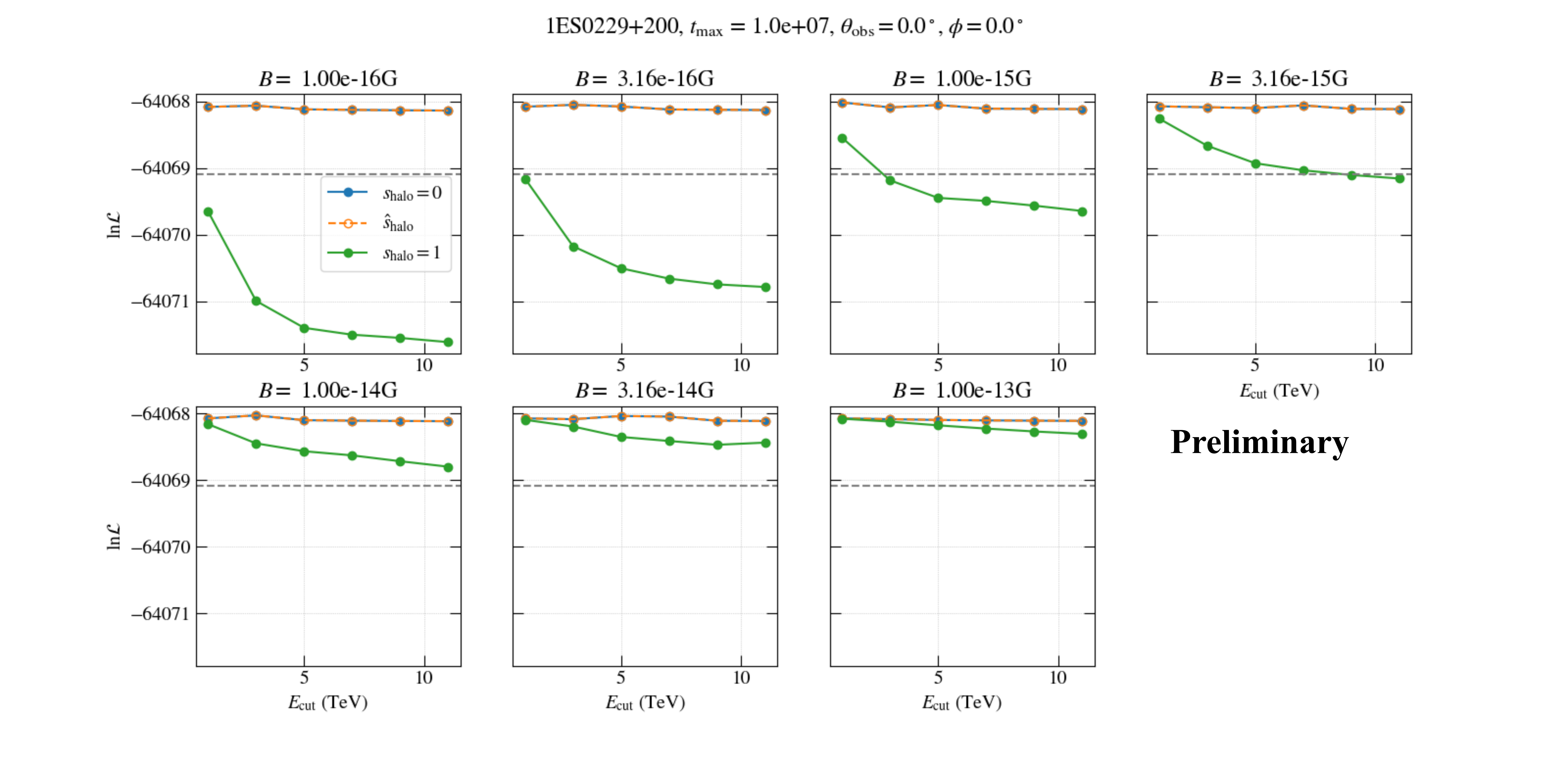

H.E.S.S.

Fermi-LAT Analysis with halo component — Examples of likelihood profile with Γ